Wear 368-369 (2016) 350–357

Contents lists available at ScienceDirect

Wear

journal homepage: www.elsevier.com/locate/wear

Load-dependent run-in and wear behaviour of line-like surface patterns produced by direct laser interference patterning

Andreas Rosenkranz *, Joris C. Pangraz, Carsten Gachot, Frank Mücklich

Saarland University, Department of Materials Science and Engineering, Campus, 66123 Saarbrücken, Germany

ARTICLE INFO

Article history:
Received 29 June 2016
Received in revised form
7 October 2016
Accepted 13 October 2016
Available online 15 October 2016

Keywords:
Laser surface patterning
Dry friction
Run-in behaviour
Sliding wear

ABSTRACT

Line-like patterns having periodicities of 6 and 9 μm as well a structural depth of 1 μm were created by direct laser-interference patterning on stainless steel substrates (AISI-304). Dry sliding tests using a ball-on-disk configuration were performed under dry sliding in order to study the run-in behaviour of these samples as a function of the applied normal load (0.5, 1, 10 and 15 mN) and the ball diameter (3 and 6 mm). The resulting wear tracks were examined by light microscopy, white light interferometry and scanning electron microscopy in order to study the underlying friction and wear mechanisms. Dependent on the applied normal load, clear differences in the frictional behaviour can be observed. For small normal loads (0.5 and 1 mN), the underlying friction and wear mechanism seems to be adhesion-dominated while for 10 and 15 mN, plastic deformation and abrasion are the most important contributions. It could be shown that, for small normal loads, the surface pattern with a periodicity of 6 μm leads to a significant reduction of the initial and final COF by a factor of roughly 2 and 4, respectively. Regarding the wear performance, no beneficial effects of the laser-patterning could be observed.

1. Introduction

Specific surface features induced by surface texturing can be used to tailor the optical, antimicrobial or tribological properties of surfaces [1–5]. Regarding the tribological performance, numerous research articles have demonstrated the beneficial performance of these surface features under different lubricated conditions. Depending on the respective lubrication regime, the entrapment of wear debris [5,6], the storage of additional oil in order to act as a secondary oil source [5,7,8], the build-up of an additional hydrodynamic pressure [5,9,10], the reduction of the contact area [3,4] and stiction [11] can be named as possible beneficial mechanisms thus improving the friction and wear properties.

In the case of dry friction, a lot of publications have been focused on the entrapment of the produced wear particles to avoid third body interactions or to enhance the performance of magnetic storage disks due to reduced stiction [12–16]. Borghi et al. combined nitriding and laser-texturing for steel samples. They could prove that the coefficient of friction (COF) can be reduced by roughly 10%. This was attributed to the entrapment of wear particles in the surface features [17]. In addition to that, Rapoport investigated the effect of solid lubricants on laser-patterned steel samples. These authors could prove an enhanced tribological behaviour of these surfaces which was explained by an improved storage of solid lubricant due to laser-patterning [14].

Besides the influence of the pattern diameter, periodicity, depth or area density, alignment effects on the resulting COF needs to be considered (relative alignment of the pattern with respect to the sliding direction of the counter body). Gachot et al. produced by direct laser interference patterning (DLIP) line-like surface patterns with three different periodicities, namely 5, 9 and 18 μm, and a structural depth of roughly 1 μm on the substrate as well as on the tribological counter body [3,18]. The authors concluded that the alignment plays an important role with respect to the resulting frictional properties. However, this was just demonstrated for 200 sliding cycles. Consequently, Rosenkranz et al. continued this work thus performing experiments with up to 20.000 cycles in order to analyse degradation effects and the long-term stability of the patterned surfaces [4]. By image analysis using Fourier-transformation, they could demonstrate that the laser-patterning still exists even after 20.000 sliding cycles. Concerning the alignment effects, it could be shown that patterns oriented perpendicular to each other and to the sliding direction of the ball (named as perp- and 90° alignment in [4]) induce a reduced COF. These observations are in good agreement with the work of He et al. [19]. In this context, Yu et al. have investigated the “topographic dependence of friction on micro- and nano-grooved surfaces” [20]. Ball-on-disk experiments (ball radius R) under dry sliding conditions were performed on disks with different line patterns. The patterns were produced by laser ablation and the periodicity (width b) was

* Corresponding author.
E-mail address: a.rosenkranz@mx.uni-saarland.de (A. Rosenkranz).

http://dx.doi.org/10.1016/j.wear.2016.10.008
0043-1648/

varied between 139 nm to 110 μm. Under the assumption of negligible wear, the effect of contact area, stiction length, energy barrier and contact stiffness was discussed dependent on the relative alignment [20].

In this work, we study the load-dependent run-in and wear behaviour of line-like surface patterns produced by DLIP on stainless steel under dry sliding using. The tribological experiments were performed on a ball-on-disk tribometer in linear reciprocating sliding mode as a function of the applied normal load (ranging from 0.5 up to 15 mN), the ball diameter (3 and 6 mm) and the pattern periodicity (6 and 9 μm). These periodicities were selected because of two main reasons. Smaller periodicities in the range between 5 and 12 μm can be fabricated with a high precision and homogeneity due to negligible interactions of two adjacent interference maxima positions. Additionally, as demonstrated in previous publications, surface patterns with smaller periodicities tend to have an improved tribological behaviour and a reduced COF [3,4]. Additionally, the pattern orientation was chosen to be perpendicular with respect to the sliding direction of the ball since in a previous manuscript, it could be shown that this orientation leads to a reduced COF [4]. After the tribological experiments, the resulting wear tracks were examined by light microscopy, white light interferometry (WLI) and scanning electron microscopy (SEM) in order to study the underlying friction and wear mechanisms. In addition to that, the wear volumes were estimated based upon cross-sectional plots recorded by WLI. As a consequence, this manuscript can be understood as a follow-up paper of our previous published work in this journal. Therefore, all experimental conditions and parameters were kept constant in order to allow for a direct comparison with the previous results.

2. Experimental procedure

Commercially available, stainless steel substrates ($20 \times 20 \times 1$ mm^3 AISI-304) with a highly-polished surface finish ($R_q \sim 30$ nm) were laser-patterned. The tribological experiments were performed using Alumina balls having a diameter of 3 and 6 mm. Alumina balls were selected due to their high hardness thus avoiding any influence of plastic deformation of the counter body. The chemical composition of the steel is summarised in Table 1 (supplier information and checked by energy dispersive X-ray spectroscopy).

DLIP was done using a pulsed solid-state Nd:YAG laser (Spectra Physics, Quanta Ray PRO 290) producing pulses with a duration of 10 ns and a wavelength of 355 nm (third harmonic). The patterning was performed under normal atmospheric conditions (room temperature and atmospheric pressure). A beam splitter is used to split the primary laser beam into "two sub-beams which interfere on the sample surface resulting in a line-like pattern" [21,22]. The pattern periodicity, being the distance between two adjacent topographical peaks, is a characteristic parameter of the produced pattern. The periodicity can be changed by varying the wavelength of the laser or the angle between the sub-beams [21,22]. Two different periodicities, namely 6 and 9 μm, were selected for the tribological experiments. The laser fluence was kept constant at 29 J/cm^2 for all samples in order to generate homogeneous surface patterns. Further details concerning the laser patterning process and the experimental set-up as well as the laser-matter interaction have been already published elsewhere [21,22].

Table 1
Chemical composition of the steel substrate in wt% (specification provided by the supplier and checked by energy dispersive X-ray spectroscopy).

Specimen	Fe	Cr	Ni	Mn	Si	C
Steel (AISI 304)	68.9	18	10	2	1	0.1

Table 2
Calculated contact area and contact pressure according to the Hertzian contact model as a function of the ball diameter and the applied normal load.

Ball diameter (mm)	Normal load (mN)	Calculated contact area (μm^2)	contact pressure (MPa)
3	0.1	2.700	55.6
	1	12.533	119.7
	10	58.175	257.8
	15	76.230	295.2
6	0.1	4.286	35
	1	19.896	75.4
	10	92.347	162.4
	15	121.008	185.9

For the tribological experiments, a nanotribometer (CSM Instruments) using a ball-on-disk configuration in a linearly reciprocating sliding mode with a stroke length of 0.6 mm and a sliding speed of 1 mm/s was utilized. The sampling rate of the friction tests was 100 Hz (100 data points per second). The respective velocity profile is a sinusoidal function with a maximum speed of 1 mm/s in the middle of the stroke.

The normal load was varied between 0.5 and 15 mN in order to study the load-dependency of the run-in and wear behaviour. The resulting contact area and contact pressure as a function of the applied load and ball diameter are summarized in Table 2 and graphically depicted in Fig. 1. The number of cycles was kept constant at 200 (6 min measuring time) as in our previous publication [4]. Due to the anisotropy of the pattern and the resulting preferential orientation, the alignment of the patterned samples needs to be considered. The sliding direction of the ball was perpendicular with respect to the preferential orientation of the pattern. This was also chosen based upon our previous research work showing that this alignment leads to a reduced COF [4]. In order to ensure a precise alignment of the laser-patterned sample, the same positioning method for single-sided patterned surfaces as described in [4] was used. A stiff cantilever which acts as a frictionless force transducer in both vertical and horizontal directions holds the Alumina ball. The cantilever is loaded onto the substrate using piezo actuation in order to precisely adjust the normal load. During the experiment, the deflection of the elastic arms in both directions is measured by optical fibre displacement sensors. The stiffness in both directions is known (normal stiffness $=0.1536\ \frac{\text{mN}}{\mu\text{m}}$, lateral stiffness $=0.2094\ \frac{\text{mN}}{\mu\text{m}}$). Accordingly, the normal and friction force as well as the COF can be easily calculated. Finally, the mean value for each sliding cycle was calculated from the absolute measured raw values of one forward and backward motion, excluding the data obtained at the reversal points. Temperature and relative humidity were kept constant at 20 ± 2 °C and 4 ± 0.5%, respectively. Finally, it is worth mentioning that each tribological experiment (for each parameter such as normal load, ball diameter and periodicity) was repeated ten times in order to estimate the respective mean values and standard deviations.

The topography of the modified surfaces and the resulting wear tracks were measured by WLI (Zygo New View 7300), optical microscopy (light microscope Olympus BX 60) and SEM (FEI Strata DB 235). Using cross-sectional measurements performed by WLI, the respective wear volumes were estimated.

3. Results and discussion

The tribological tests under dry sliding conditions were performed to investigate the load-dependent run-in and wear behavior

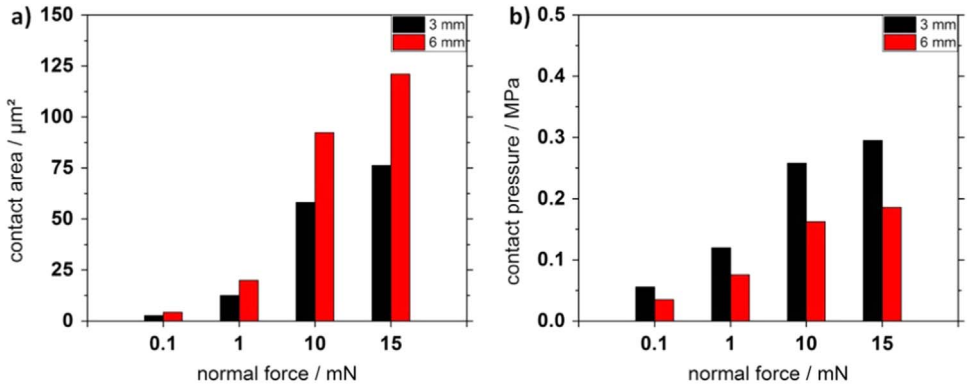

Fig. 1. Estimated contact area (a) and contact pressure (b) according to the Hertzian contact model as a function of the ball diameter and the applied normal load.

of the polished reference and laser-patterned surfaces as a function of the ball diameter. In order to demonstrate the influence of the experimental conditions, the Hertzian contact area and contact pressure for the polished reference were estimated taking all normal loads and ball diameters into consideration. As can be seen in Fig. 1 and Table 2, the normal load and the ball diameter significantly influence the resulting contact area and contact pressure. For example, for a normal load of 0.5 mN and a ball diameter of 3 mm, the resulting contact area is approximately 2.7 μm^2, whereas the contact area increases by a factor of 6 (76 μm^2) for 15 mN. This leads to the conclusion that the run-in and wear behavior may be significantly affected by the different experimental conditions.

First, tribological reference measurements with a polished, unpatterned steel substrate and an Alumina ball were performed as a function of the applied normal load and ball diameter.

The temporal evolutions of the COF depicted in Fig. 2 reveal clear differences with respect to the run-in behaviour dependent on the applied normal load. It is evident that tribological experiments with 0.5 and 1 mN as well as experiments with 10 and 15 mN tend to have a similar run-in behaviour.

The frictional curves of the experiments performed with smaller normal loads typically start around 0.4 or 0.6 and show an increase in the following sliding cycles. Afterwards, the COF slightly decreases (3 mm ball diameter) or remains fairly constant (6 mm ball diameter). Taking the given standard deviations into consideration, it can be stated that the temporal evolutions of the COF measured for small normal loads are very similar due to the partial overlap of the error bars. According to Blau who classified the run-in behaviour in eight different curves, the observed curve is typical for a "dry, non-lubricated metal contact with a small amount of surface contamination or a thin oxide scale" [23]. Besides the surface chemistry, also the surface roughness can affect the frictional behaviour. This can lead to a certain increase in the COF until "surface conformity and smoothing occur" [23]. In a previous publication [4], the run-in behaviour of polished samples and line-like surface patterns dependent on the relative alignment has been studied in detail for a normal load of 1 mN. The general shape of those curves for the polished samples is pretty similar. Consequently, a more detailed discussion about the contributing factors and the frictional behaviour of the polished reference can be found in [4]. In addition to that, this figure also shows that some curves haven't reached steady-state conditions after 200 sliding cycles. The long term behaviour of the line-like surface patterns for low normal loads (1 mN) has also already been addressed in [4]. For a detailed discussion of involved effects and phenomena, please refer to [4].

In contrast to that, the temporal evolutions of the COF measured for 10 and 15 mN demonstrate a completely different behaviour. The initial COF is around 0.25. Afterwards, the COF rapidly increases irrespective of the used ball diameter thus reaching a COF of roughly 0.87 and 0.75 for a ball diameter of 3 and 6 mm, respectively. According to Blau, sharp transitions in the COF can be well correlated with a degradation of the oxide layer thus producing abrasive wear particles and severe plastic deformation as well as abrasive wear [23–26].

From the literature, it is very well known that adhesion (μ_a), deformation (μ_d) and wear particles (μ_{dp}) contribute to the determined COF [27–29]. The material pairing and contact area are the main influencing factors for μ_a [27]. The degree of plastic deformation needs to be considered with regard to μ_d [27]. Based upon the presented frictional curves, the contributions to the COF and the classification of the run-in behaviour according to Blau, it can be assumed that the same friction and/or wear mechanisms may act for 0.5 and 1 mN as well as for 10 and 15 mN. Furthermore,

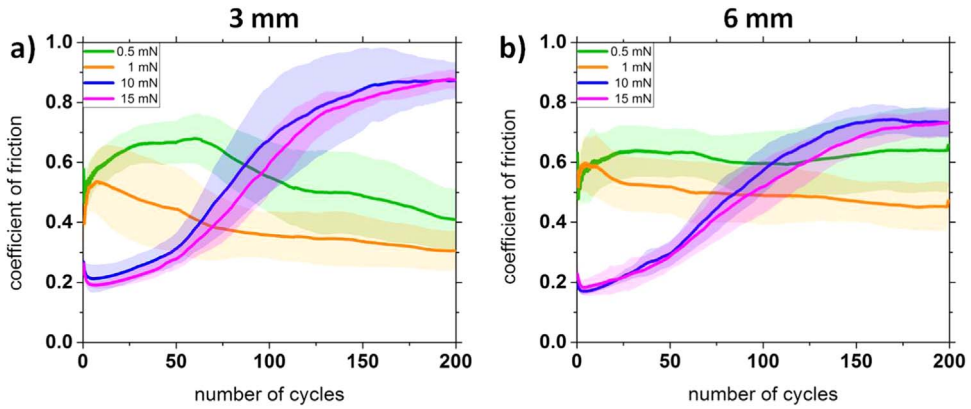

Fig. 2. Temporal evolution of the COF of the polished reference as a function of the applied normal load for a ball diameter of 3 (a) and 6 mm (b).

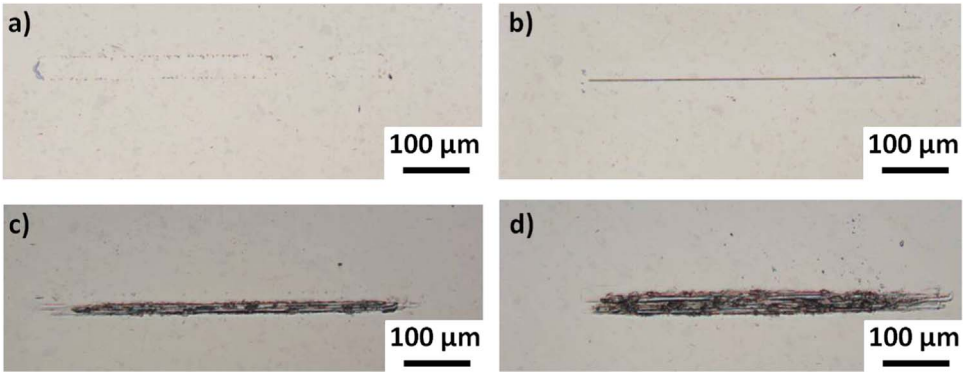

Fig. 3. Light-microscopic images recorded of the resulting wear tracks of the polished reference sample after 200 sliding cycles with a normal load of 0.5 (a), 1 (b), 10 (c) and 15 mN (d).

it can be assumed that the friction/wear mechanisms for smaller normal loads are dominated by adhesion whereas the deformation and wear particles component might predominate for 10 and 15 mN.

In order to prove these assumptions and to study the underlying mechanisms, the resulting wear tracks of the polished reference were imaged by light microscopy. The corresponding wear tracks as a function of the normal load are depicted in Fig. 3.

Similar to the presented friction curves, the resulting wear tracks demonstrate clear differences dependent on the used normal load. For 0.5 and 1 mN (Fig. 3a and b), almost no wear track is visible and just some very tiny wear features can be observed. Due to the lack of severe wear features for these normal loads, it can be concluded that the frictional behaviour is mostly influenced by adhesion and consequently by the contact area. In contrast to that, very well pronounced wear scars with severe wear marks can be noticed for 10 and 15 mN (Fig. 3a and b). Consequently, the friction and wear behaviour are mainly affected by plastic deformation and abrasion as well as the influence of produced wear particles. Based upon this figure, it is visible that the resulting wear track width increases with increasing normal load which seems to be reasonable due to the increased contact area (please refer to Fig. 1 and Table 2). Additionally, it is worth mentioning that the light-microscopic images were taken after cleaning the samples in an ultrasonic bath. Before that, wear particles are clearly visible in the wear track as well as in close proximity around the wear track.

After the laser patterning, the resulting surface roughness was characterised by WLI and the respective results are given in Table 3. Based upon this table, it is visible that the structural depth of both patterned samples (indicated by the Swedish Height H) is very similar. Additionally, it is well noticeable that the laser patterning leads to an increase in the surface roughness indicated by R_a and R_q.

Fig. 4 summarizes the temporal evolutions of the COF for a line-like surface pattern with a periodicity of 6 µm as a function of the applied normal load and ball diameter.

As can be seen in Fig. 4, similar trends regarding the load-dependent run-in behaviour as discussed before for the polished reference can be observed for the line-like pattern with a periodicity of 6 µm. It is interesting to notice that all frictional curves irrespective of the applied normal load and ball diameter start at roughly the same COF of around 0.3. The frictional curves for a normal load of 0.5 and 1 mN demonstrate firstly a certain decrease in the COF. Subsequently, a slight increase in the COF over time can be noticed. The analysis of the resulting wear tracks by SEM demonstrates some flattening taking place at the topographic maxima positions as can be seen in Fig. 5a and b. Consequently, the observed frictional behaviour can be well correlated with the flattening of the highest asperities as well as with some plastic deformation thus inducing some degradation of the laser-pattern. This can lead to a slight increase in the real contact area. This is a good agreement with our previous publication in Wear [4].

In contrast to that, the frictional curves for normal loads of 10 and 15 mN start roughly at the same initial COF value, but show a sharp increase in the COF. After approximately 200 sliding cycles, the curves (10 and 15 mN) stabilize around 0.9 (3 mm ball diameter) and 0.8 (6 mm ball diameter). The observed change in the COF can be directly correlated with severe abrasion thus leading to the complete destruction of the surface pattern (Fig. 5c and d). This degradation going hand in hand with a change in the surface topography can also be seen in the white light interferometric and light microscopic images of the resulting wear tracks depicted in Fig. 6.

Moreover, the removal of the oxide layer induces a change from an oxide-oxide to a metal-oxide contact situation which is surely another influencing factor contributing to the observed behaviour. The fact that the frictional curves (10 and 15 mN) end up in roughly the same COF suggests that the frictional behaviour after 200 sliding cycles do not longer depend on the produced surface pattern and the initial oxide layer after laser patterning. It is worth mentioning that the error bars for larger normal loads are more pronounced than for smaller normal loads. This can be explained by the formation of wear particles and the larger degree of plastic deformation due to higher normal loads thus leading to a more inhomogeneous surface and affecting the tribological behaviour in a more stochastic way. Furthermore, the oxide layer does not have a uniform thickness, which results also in a larger spread of the COF and thus to larger standard deviations. This agrees very well with our previous publication [4] in which we have studied the long term behaviour of line-like surface patterns dependent on the respective relative alignment for a normal load of 1 mN. The observed temporal evolution could be explained by the removal of the oxide layer, the degradation of the surface pattern und the formation of wear particles. Consequently, a higher normal load increase the probability to form wear particles and make the destruction of the surface pattern as well as the removal of the oxide layer more likely. Thus, the transition will occur earlier for a lower number of sliding cycles.

Fig. 7 summarizes the temporal evolutions of the COF for a line-

Table 3
Roughness parameters R_a, R_q and H measured by WLI for the reference and the laser-patterned samples with different periodicities.

Sample	R_a (µm)	R_q (µm)	H (µm)	P (µm)
Reference	0.012 ± 0.004	0.014 ± 0.004	0.046 ± 0.011	/
P 6	0.289 ± 0.083	0.339 ± 0.092	0.778 ± 0.253	6.172 ± 0.128
P 9	0.390 ± 0.038	0.459 ± 0.046	0.875 ± 0.290	8.835 ± 0.098

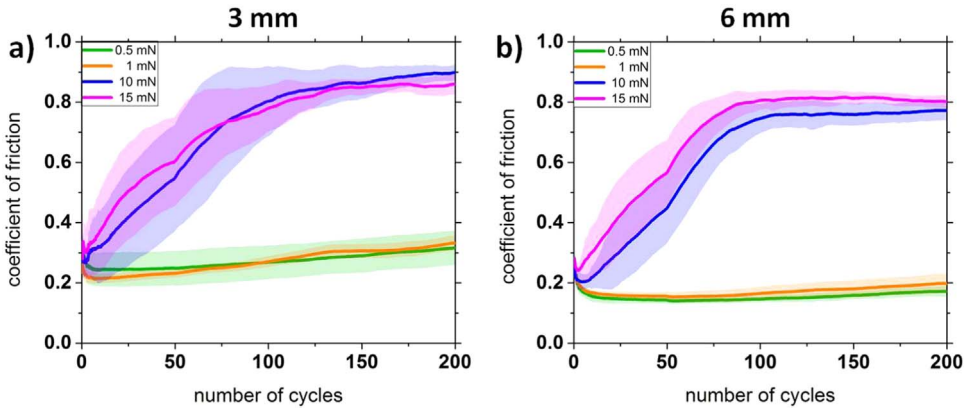

Fig. 4. Temporal evolution of the COF of the line-like surface pattern with a periodicity of 6 μm as a function of the applied normal load for a ball diameter of 3 (a) and 6 mm (b).

like surface pattern with a periodicity of 9 μm as a function of the applied normal load and ball diameter.

Similar trends as observed for the load-dependent run-in behaviour of the line-like pattern with a periodicity of 6 μm can be seen in Fig. 7. The initial COF of all frictional curves lies between 0.25 and 0.32. Afterwards, the COF for normal loads of 0.5 and 1 mN slightly drops down and finally shows a slight increase or remains nearly constant at values between 0.23 and 0.28. The observed frictional behaviour can be explained by the flattening and plastic deformation of the laser-pattern. The frictional curves for normal loads of 10 and 15 mN start roughly at the same initial COF, but show a sudden increase afterwards. After approximately 200 sliding cycles, both curves (10 and 15 mN) tend to stabilize at values around 0.7 and 0.8. The observed change in the COF can be again correlated with the complete destruction of the surface patterning. This can be clearly seen in the white light interferometric and light microscopic images of the resulting wear tracks depicted in Fig. 8.

As for the pattern with a periodicity of 6 μm, not only the degradation of the surface pattern, but also the removal of the oxide layer changing the contact situation needs to be considered as possible contributions.

Table 4 summarizes the initial and final (after 200 sliding cycles) COF for all measured samples in order to allow for a better comparison of the resulting frictional response.

For the polished reference, similar values for the initial and final COF can be found for the small and high normal loads irrespective of the ball diameter. In the case of higher normal loads (10

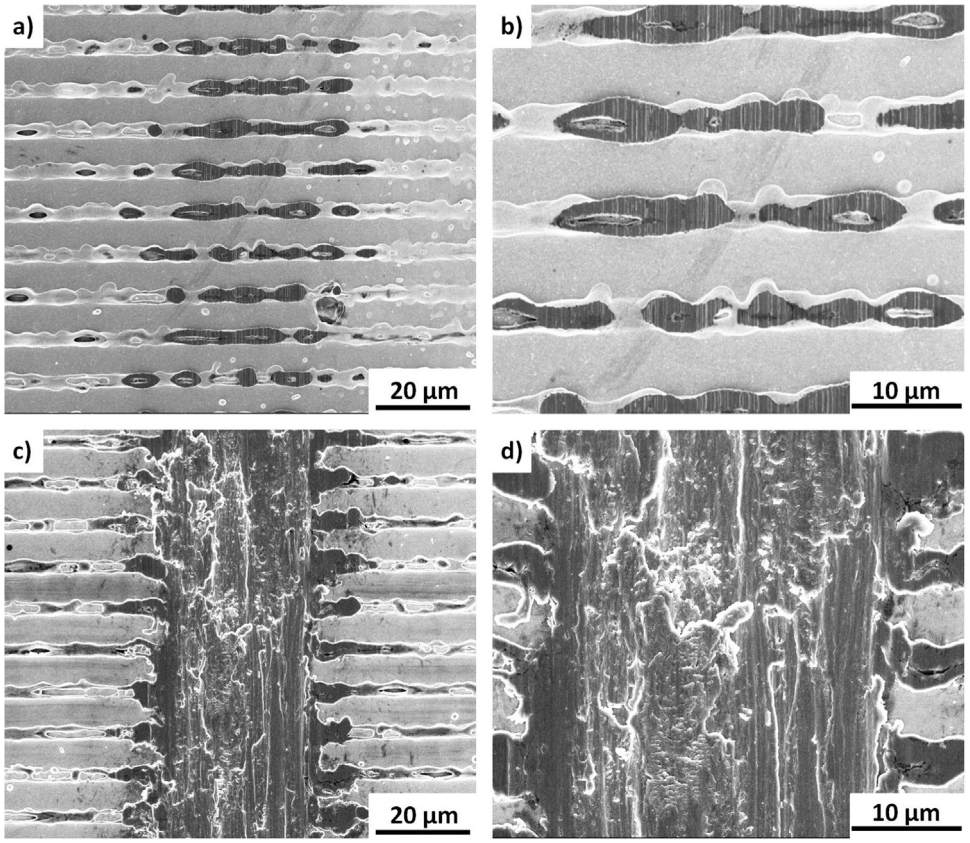

Fig. 5. SEM-micrographs with two different magnifications of the respective wear tracks detected on the line-like surface pattern with a periodicity of 9 μm for 1 (a) and (b) and 15 mN (c) and (d).

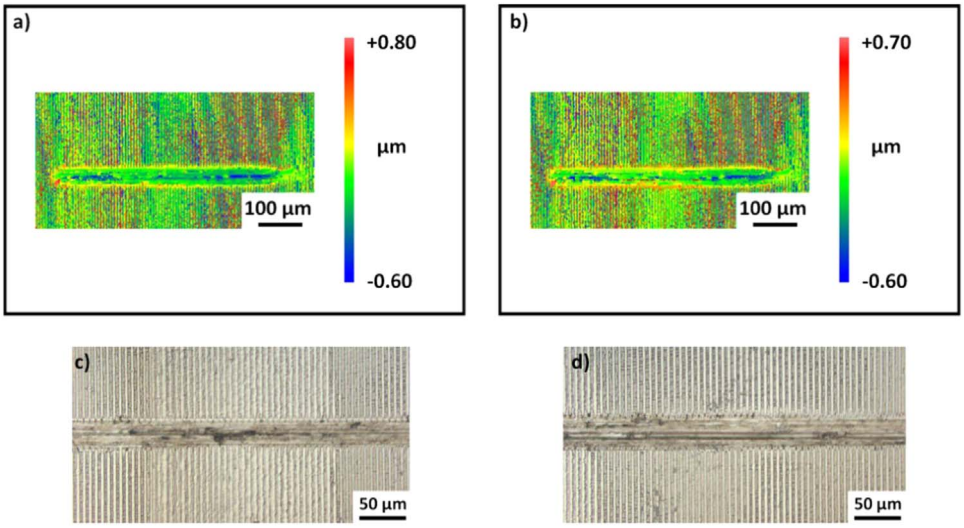

Fig. 6. White light interferometric (a) and (b) and light microscopic images (c) and (d) of the resulting wear tracks of the line pattern with a periodicity of 6 µm for 10 (a) and (c) and 15 mN (b) and (d). The laser-patterned surfaces (a) and (b) seem to be blurred with a reduced homogeneity. This can be traced back to the larger scale bar thus leading to a decreased resolution in order to display the entire wear track.

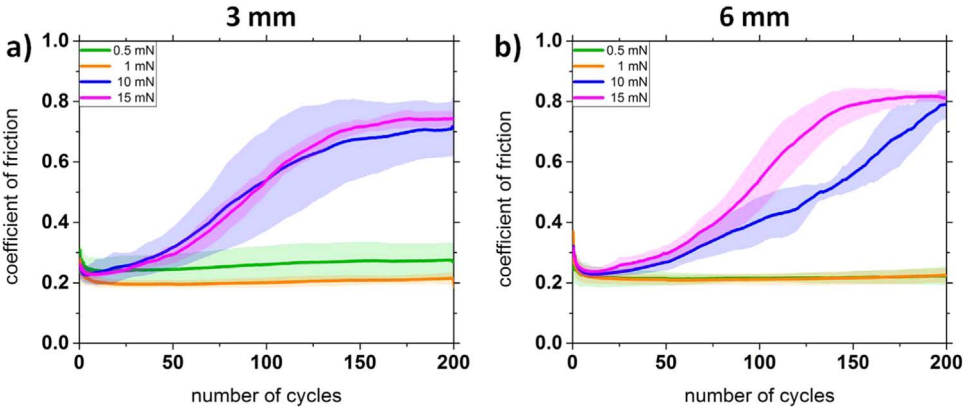

Fig. 7. Temporal evolution of the COF of the line-like surface pattern with a periodicity of 9 µm as a function of the applied normal load for a ball diameter of 3 (a) and 6 mm (b).

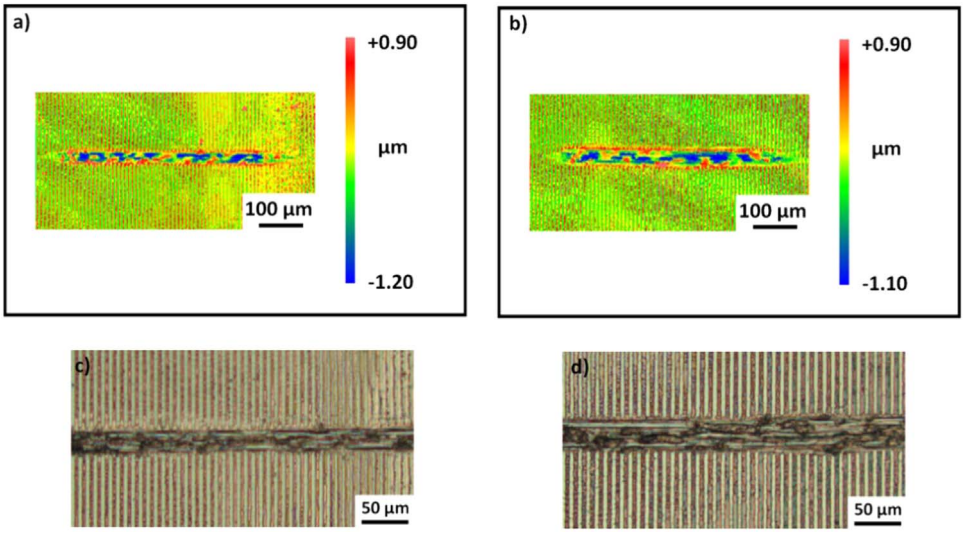

Fig. 8. White light interferometric (a) and (b) and light microscopic images (c) and (d) of the resulting wear tracks of the line pattern with a periodicity of 9 µm for 10 (a) and (c) and 15 mN (b) and (d). The laser-patterned surfaces (a) and (b) seem to be blurred with a reduced homogeneity. This can be traced back to the larger scale bar thus leading to a decreased resolution in order to display the entire wear track.

Table 4
Summary of the initial and final COF for the polished reference and the laser-patterned surface with different periodicities dependent on the applied normal load and ball diameter.

Ball diameter	Sample	COF	0.5 mN	1 mN	10 mN	15 mN
3 mm	Ref	μ_{ini}	0.57 ± 0.14	0.41 ± 0.10	0.26 ± 0.03	0.26 ± 0.03
		μ_{end}	0.41 ± 0.10	0.30 ± 0.06	0.88 ± 0.06	0.88 ± 0.03
	Line-pattern 6 μm	μ_{ini}	0.33 ± 0.05	0.25 ± 0.03	0.25 ± 0.06	0.25 ± 0.03
		μ_{end}	0.31 ± 0.05	0.33 ± 0.02	0.89 ± 0.02	0.85 ± 0.03
	Line-pattern 9 μm	μ_{ini}	0.30 ± 0.05	0.27 ± 0.06	0.24 ± 0.05	0.24 ± 0.04
		μ_{end}	0.21 ± 0.06	0.21 ± 0.02	0.70 ± 0.09	0.74 ± 0.03
6 mm	Ref	μ_{ini}	0.63 ± 0.07	0.57 ± 0.11	0.19 ± 0.02	0.22 ± 0.04
		μ_{end}	0.63 ± 0.13	0.45 ± 0.05	0.73 ± 0.05	0.73 ± 0.04
	Line-pattern 6 μm	μ_{ini}	0.28 ± 0.03	0.26 ± 0.03	0.25 ± 0.04	0.28 ± 0.04
		μ_{end}	0.17 ± 0.02	0.19 ± 0.03	0.77 ± 0.03	0.80 ± 0.02
	Line-pattern 9 μm	μ_{ini}	0.21 ± 0.10	0.21 ± 0.07	0.31 ± 0.04	0.31 ± 0.08
		μ_{end}	0.32 ± 0.03	0.32 ± 0.02	0.78 ± 0.05	0.81 ± 0.02

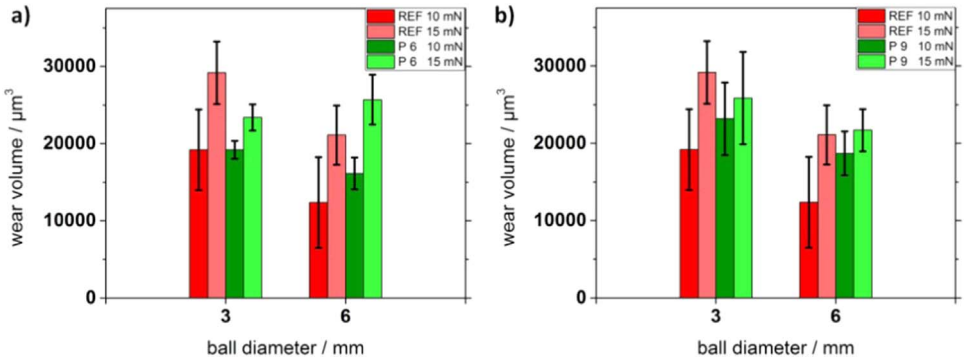

Fig. 9. Comparison of the estimated wear volumes based upon the WLI measurements of the polished reference and the laser-patterned surfaces with 6 (a) and 9 μm periodicity (b) as a function of the ball diameter and the applied load.

and 15 mN), the initial and final COF of the polished reference and laser-patterned surface are very similar and no beneficial effect of the patterning can be noticed. This can be explained by severe plastic deformation and abrasion induced by higher normal loads. This leads to the complete destruction of the laser pattern and the effect of the surface pattern vanishes.

However, for small loads (0.5 and 1 mN), both surface patterns (6 and 9 μm periodicity) significantly reduce the initial and final COF compared to the polished reference. The maximum friction reduction with respect to the initial and final COF can be observed for the line-like pattern with a periodicity of 6 μm (measured with a ball diameter of 6 mm and a normal load of 0.5 mN). The initial COF for this surface pattern is reduced by a factor of 2.25 while the final COF after 200 sliding cycles shows an improvement of a factor of 3.7. Those results are in very good agreement with previous published research work by the authors showing a more pronounced friction reduction for smaller periodicities [3,4,18]. In addition to that, Gachot et al. (in collaboration with co-workers from the Imperial College) performed some numerical simulations discussing the influence of the pattern periodicity [30]. In this study, they could demonstrate that smaller periodicities lead to a reduced contact area thus significantly lowering the resulting COF. This matches quite well with the obtained trend that the largest friction reduction is observed for the smaller pattern periodicity.

The resulting wear volumes for the polished reference and the laser-patterned surfaces for normal loads of 10 and 15 mN were estimated based upon white light interferometric images (displayed in Figs. 6 and 8) and cross-section plots. Since there are almost no visible wear scars in the case of smaller normal loads, no wear volume could be estimated by WLI for 0.5 and 1 mN. For 10 and 15 mN, the respective wear track width and depth were measured ten times by WLI and the averaged values were multiplied by the wear track length (600 μm) in order to estimate the wear volume. However, it should be mentioned that this is just an approximation of the resulting wear volume since the respective wear track shape is assumed to be circular (circular segment). The results of this analysis are summarized in Fig. 9 as a function of the applied normal load and the ball diameter.

Considering the mean values and the respective standard deviations, it is clearly noticeable that the laser-patterned surfaces do not lead to an improved wear performance irrespective of the adjusted periodicity. As already discussed, this can be explained by the severe plastic deformation and abrasive wear thus completely destroying the laser-patterns for these normal loads. With regard to the ball diameter and the applied normal load, no significant difference between the polished reference and the laser-patterned surface can be seen.

4. Conclusions

The aim of this study was to study the load-dependent run-in and wear behaviour of line-like patterns with different periodicities (6 and 9 μm) fabricated by DLIP. For this purpose, dry sliding tests were performed on a ball-on-disk tribometer using four different normal loads and two ball diameters. In order to analyse the respective frictional and wear response, the temporal evolution of the COF was discussed in detail. Additionally, the resulting wear tracks were examined by light microscopy, white light interferometry and scanning electron microscopy in order to characterise the underlying friction and wear mechanisms. Dependent on the applied normal load, clear differences in the temporal evolution of the COF and consequently in the run-in as well as wear behaviour can be observed. For small normal loads (0.5 and

1 mN), the underlying friction and wear mechanism is adhesion-dominated. In the case of higher normal loads (10 and 15 mN), plastic deformation and abrasion are the most important contributions. In terms of friction reduction, the laser patterning was only effective when using small normal loads (0.5 and 1 mN). In this context, the surface pattern with a periodicity of 6 μm (ball diameter of 6 mm) revealed the most pronounced friction reduction (initial and final COF) by a factor of 2.2 and 3.7, respectively. For higher normal loads (10 and 15 mN), no beneficial effects regarding a possible friction reduction could be observed due to the complete degradation of the laser-pattern under these contact pressures. Regarding the wear volume and the respective wear performance, no beneficial effects of the laser patterning could be observed.

Acknowledgements

The present work is supported by funding from the Deutsche Forschungsgemeinschaft in the priority program SPP 1551 “Resource efficient design elements” (DFG, project: MU 959/27-1/2). The EU funding for the project AME-Lab (European Regional Development Fund C/4-EFRE-13/2009/Br) is gratefully acknowledged. Dr. S. Suarez and P. G. Grützmacher are kindly acknowledged for proof-reading.

References

[1] L. Müller-Meskamp, Y.H. Kim, T. Roch, S. Hofmann, R. Scholz, S. Eckardt, A. F. Lasagni, Efficiency enhancement of organic solar cells by fabricating periodic surface textures using direct laser interference patterning, Adv. Mater. 24 (2012) 906–910.
[2] S. Mathews, M. Hans, F. Mücklich, M. Solioz, Contact killing of bacteria on copper is suppressed if bacterial-metal contact is prevented and is induced on iron by copper ions, Appl. Environ. Microbiol. 79 (2013) 2605–2611.
[3] C. Gachot, A. Rosenkranz, L. Reinert, E. Ramos-Moore, N. Souza, M.H. Müser, F. Mücklich, Dry friction between laser-patterned surfaces: role of alignment, structural wavelength and surface chemistry, Tribol. Lett. 49 (2013) 193–202.
[4] A. Rosenkranz, L. Reinert, C. Gachot, F. Mücklich, Alignment and wear debris effects between laser-patterned steel surfaces under dry sliding conditions, Wear 318 (2014) 49–61.
[5] A. Rosenkranz, T. Heib, C. Gachot, F. Mücklich, Oil film lifetime and wear particle analysis of laser-patterned stainless steel surfaces, Wear 334 (2015) 1–12.
[6] U. Pettersson, S. Jacobson, Influence of surface texture on boundary lubricated sliding contacts, Tribol. Int. 36 (2003) 857–864.
[7] G. Dumitru, V. Romano, H.P. Weber, H. Haefke, Y. Gerbig, E. Pflueger, Laser microstructuring of steel surfaces for tribological applications, Appl. Phys. A 70 (2000) 485–487.
[8] S. Wos, W. Koszela, P. Pawlus, Determination of oil demand for textured surfaces under conformal contact conditions, Tribol. Int. 93 (2016) 602–613.
[9] H.L. Costa, I.M. Hutchings, Hydrodynamic lubrication of textured steel surfaces under reciprocating sliding conditions, Tribol. Int. 40 (2007) 1227–1238.
[10] M.T. Fowell, A.V. Olver, A.D. Gosman, H.A. Spikes, I. Pegg, Entrainment and inlet suction: two mechanisms of hydrodynamic lubrication in textured bearings, J. Tribol. 129 (2007) 336–347.
[11] P. Baumgart, D.J. Krajnovich, T.A. Nguyen, A.C. Tam, A new laser texturing technique for high performance magnetic disk drives, IEEE Trans. Mag. 31 (1995) 2946–2951.
[12] H. Ishihara, H. Yamagami, T. Sumiya, T. Okudera, M. Inada, A. Terada, Contact start/stop characteristics of photolithography magnetic recording media, Wear 172 (1994) 65–72.
[13] R. Ranjan, D.N. Lambeth, M. Tromel, P. Goglia, Y. Li, Laser texturing for low-flying-height media, J. Appl. Phys. 69 (1991) 5745–5747.
[14] L. Rapoport, A. Moshkovich, V. Perfilyev, I. Lapsker, G. Halperin, Y. Itovich, I. Etsion, Friction and wear of MoS_2 films on laser textured steel surface, Surf. Coat. Technol. 202 (2008) 3332–3340.
[15] M. Nosonovsky, B. Bhushan, Multiscale friction mechanisms and hierarchical surfaces in nano- and biotribology, Mater. Sci. Eng. R. 58 (2007) 162–193.
[16] S.K. Chilamakuri, B. Bhushan, Optimization of asperities for laser-textured magnetic disk surfaces, Tribol. Trans. 40 (1997) 303–311.
[17] A. Borghi, E. Gualtieri, D. Marchetto, L. Moretti, S. Valeri, Tribological effects of surface texturing on nitriding steel for high-performance engine applications, Wear 265 (2008) 1046–1051.
[18] N. Prodanov, C. Gachot, A. Rosenkranz, F. Mücklich, M.H. Müser, Contact mechanics of laser-textured surfaces, Tribol. Lett. 50 (2013) 41–48.
[19] B. He, W. Chen, Q.J. Wang, Surface texture effect on friction of a microtextured Poly(dimethylsiloxane) (PDMS), Tribol. Lett. 31 (2008) 187–197.
[20] C. Yu, H. Yu, G. Liu, W. Chen, B. He, J.Q. Wang, Understanding topographic dependence of friction with micro- and nano-grooved surfaces, Tribol. Lett. 53 (2014) 145–156.
[21] F. Mücklich, A. Lasagni, C. Daniel, Laser interference metallurgy-using interference as a tool for micro/nano structuring, Int. J. Mater. Res. 97 (2006) 1337–1344.
[22] A. Lasagni, A. Manzoni, F. Muecklich, Micro/nano fabrication of periodic hierarchical structures by multi-pulsed laser interference structuring, Adv. Eng. Mater. 9 (2007) 872–875.
[23] P.J. Blau, On the nature of running-in, Tribol. Int. 38 (2005) 1007–1012.
[24] P.J. Blau, Interpretations of the friction and wear break-in behavior of metals in sliding contact, Wear 71 (1981) 29–43.
[25] P.J. Blau, R.L. Matin, Friction and wear of carbon-graphite materials against metal and ceramic counterfaces, Tribol. Int. 27 (1994) 413–422.
[26] D. Hwang, D. Kim, S. Lee, Influence of wear particle interaction in the sliding interface on friction of metals, Wear 225 (1999) 427–439.
[27] F.P. Bowden, D. Tabor, The Friction and Lubrication of Solids, Clarendon, Oxford, 1954.
[28] D.E. Kim, N.P. Suh, On microscopic mechanisms of friction and wear, Wear 149 (1991) 199–208.
[29] B. Bhushan, M. Nosonovsky, Comprehensive model for scale effects in friction due to adhesion and two- and three-body deformation (plowing), Acta Mater. 52 (2004) 2461–2474.
[30] C. Gachot, Laser Interference Metallurgy Surfaces for Tribological Applications (Ph.D.-thesis), Saarland University, Saarbruecken, Germany, 2012.